International Journal of High-Rise Buildings
September 2018, Vol 7, No 3, 223-232
https://doi.org/10.21022/IJHRB.2018.7.3.223

International Journal of
High-Rise Buildings
www.ctbuh-korea.org/ijhrb/index.php

Load Transferring Mechanism and Design Method of Effective Detailings for Steel Tube-Core Concrete Interaction in CFT Columns with Large-Section

Yuanqi Li[1,2], Jinhui Luo[1,†], and Xueyi Fu[3]

[1]*Department of Structural Engineering, Tongji University, Shanghai 200092, China*
[2]*State Key Laboratory of Disaster Reduction in Civil Engineering, Shanghai 200092, China*
[3]*CCDI (Shenzhen), Shenzhen 518048, China*

Abstract

Two novel types of construction detailings, including using the distributive beam and the inner ring diaphragm in the joint between large-section CFT columns and outrigger truss to enhance the transferring efficiency of huge vertical load, and using the T-shaped stiffeners in the steel tube of large-section CFT columns to promote the local buckling capacity of steel tubes, were tested to investigate their working mechanism and design methods. Experimental results show that the co-working performance between steel tube and inner concrete could be significantly improved by setting the distributive beam and the inner ring diaphragm which can transfer the vertical load directly in the large-section CFT columns. Meanwhile, the T-shaped stiffeners are very helpful to improve the local bulking performance of steel tubes in the column components by the composite action of T-shaped stiffeners together with the core concrete under the range of flange of T-shaped stiffeners. These two approaches can result in a lower steel cost in comparison to normal steel reinforced concrete columns. Finally, a practical engineering case was introduced to illustrate the economy benefits achieved by using the two typical detailings.

Keywords: CFT columns with large-section, Distributive beam, Inner ring diaphragm, T-shaped stiffener, Vertical load, Local buckling

1. Introduction

In the core tube-frame-outrigger truss structural system, concrete filled steel tubular (CFT) columns with large-section bear huge vertical load together with joints between the outrigger trusses and core walls, as each outrigger truss carries huge vertical load from dozens of stories. Without special construction detailings to guarantee load transferring, it will be not sufficient for the joints to bear a huge vertical load only by the bonding force between the steel panel and core concrete, and the shear capacity of studs welded to the inner surface of the tube panels. Moreover, because the deformation of the steel tubular and core concrete may not be in accordance with the plane cross-section assumption, it would be unsafe to design large-scale section CFT columns by the current specifications. Therefore, it is critical to shorten the shear force transfer pass and guarantee the co-work behavior between the steel tube and core concrete for large-section CFT columns in practical engineering.

On the other hand, the size of large-section CFT columns is usually dominated by their stiffness requirements provided in the specification, and in order to meet the thickness to width ratio limit, the thickness of steel tubes may be larger than 80 mm, even 120 mm, especially for high-strength steel, which results in an extravagant cost of steel, i.e., the steel ratio of a large-section CFT column may be twice (approximately 10%) compared with that of a steel reinforced concrete column (approximately 5%). What more is the thick steel panel increases the difficulty of welding and quality control.

Considering the above problems in application of large-section CFT columns, and based on the summary of existing research works, a special detailing with distributive beam and inner ring diaphragm were proposed to ensure the transferring efficiency of vertical load and clarify the load pass (see Fig. 1), and the T-shaped stiffener was used to increase the local buckling capacity and reduce the steel cost of the large-section CFT columns (see Fig. 2). The load transferring mechanism and structural efficiency of these two construction detailings have been investigated by a series of tests and numerical simulations of CFT columns under axially compressing and bending-compressing load. In this paper, only the results of axially compressing tests have been introduced to highlight the efficiency of the two construction detailings due to the limita-

†Corresponding author: Jinhui Luo
Tel: +86-21-6598-3254; Fax: +86-21-6598-3431
E-mail: ljh@tongji.edu.cn

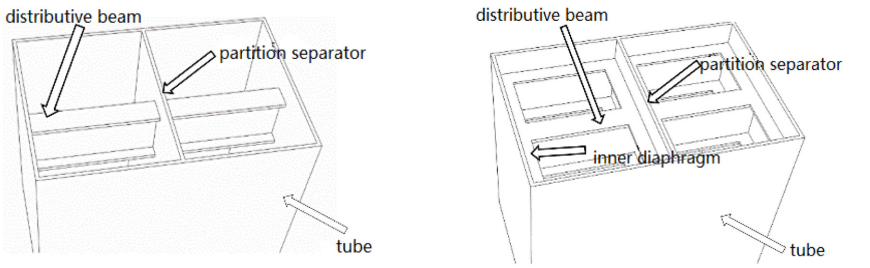

(a) Distributive beam (b) Distributive beam and inner ring diaphragm

Figure 1. Two Kinds of Vertical Load Transferring Detailings in Large-Section CFT Columns.

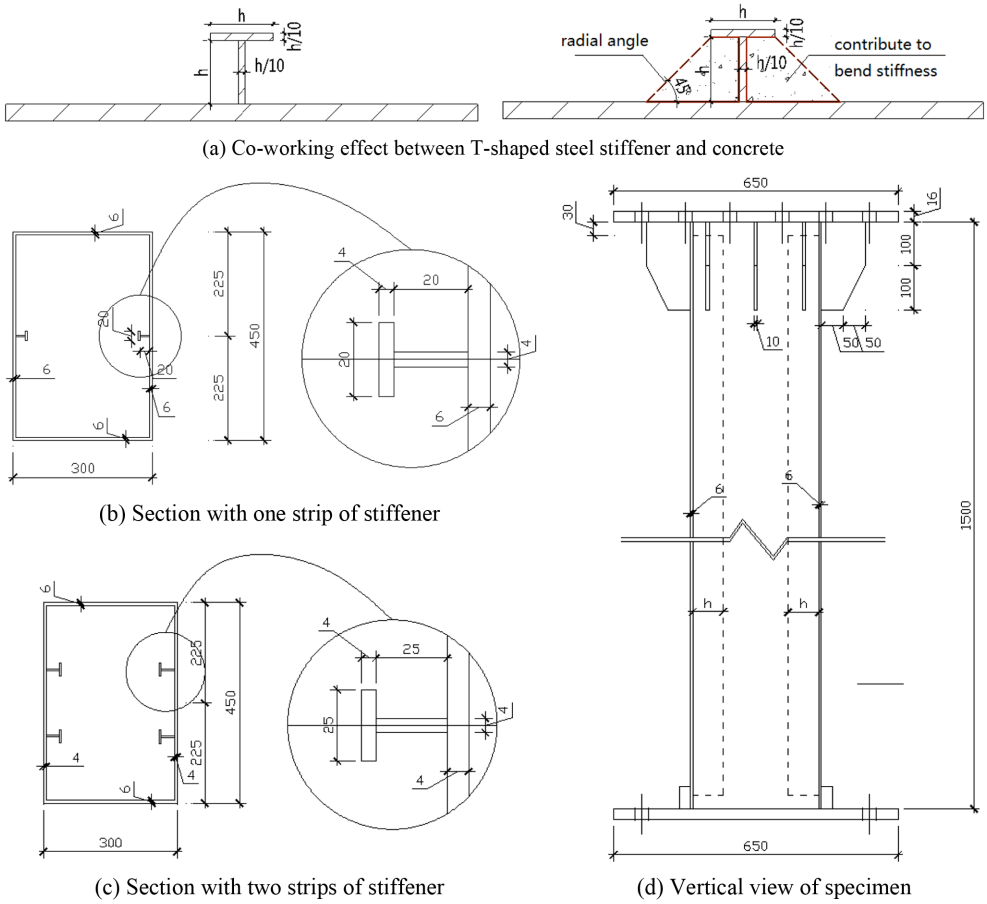

(a) Co-working effect between T-shaped steel stiffener and concrete

(b) Section with one strip of stiffener

(c) Section with two strips of stiffener (d) Vertical view of specimen

Figure 2. Specimen with T-Shaped Stiffeners.

tion of length.

2. Test Investigation of Columns with Distributive Beam and Inner Ring Diaphragm

2.1. Specimens and Test Set-up

The large-section CFT columns of a high-rise building is taken as prototype in specimen design, the large-section CFT column section is 2250 mm × 1500 mm. Three groups of scaled specimens, 15 in total, were designed with a 5:1 scaled ratio, i.e., 450 mm × 300 mm, considering different situations and parameters as shown in Table 1. The steel's grade is Q235B and the concrete's grade is C40. A special loading device was designed to apply the force directly to the outer steel tubes only in order to simulate the actual bearing situation. The top of the loading detailing is pinned to the vertical actuator.

There are two loading detailings used in the tests, LD ① for Group 1 and Group 2, and LD② for Group 3, see Fig. 3. For loading detailings LD①, a horizontal ring

Table 1. Parameters of Specimens

Group No.	Specimen No.	Section (mm)	Distributive beam (mm)	Inner ring diaphragm (mm)	Oiled	Stiffening rib	Height (mm)	Loading detailing
1	LRCFT-6-1	450×300×6	-	-	oiled	-	2700	LD ①
	LRCFT-6-2	450×300×6	-	-	-	-	2700	LD ①
	LRCFT-6-H1	450×300×6	H200×100×10×10	-	-	-	2700	LD ①
	LRCFT-6-H1+D1	450×300×6	H200×100×10×10	40×10	-	-	2700	LD ①
2	LRCFT-6-H1+D1-S	450×300×6	H200×100×10×10	40×10	-	Stiffen rib	2700	LD ①
	LRCFT-8-H1	450×300×8	H200×100×10×10	-	-	-	2700	LD ①
	LRCFT-8-H2	450×300×8	H130×70×6×6	-	-	-	2700	LD ①
	LRCFT-10-H1	450×300×10	H200×100×10×10	-	-	-	2700	LD ①
	LRCFT-10-H2-1	450×300×10	H130×70×6×6	-	-	-	2700	LD ①
3	LRCFT-10-H2-2	450×300×10	H130×70×6×6	-	-	-	2100	LD ①
	LRCFT-10-H2-3	450×300×10	H130×70×6×6	-	oiled	-	2100	LD ②
	LRCFT-10-H3-1	450×300×10	H150×100×6×8	-	oiled	-	2100	LD ②
	LRCFT-10-H3-2	450×300×10	H150×100×6×8	-	oiled	-	2100	LD ②
	LRCFT-10-H4	450×300×10	H100×50×6×6	-	oiled	-	2100	LD ②
	LRCFT-10-H5	450×300×10	H100×100×6×6	-	oiled	-	2100	LD ②

Note: Taking 'LRCFT-6-H1+D1-S' as an example, LRCFT is the abbreviation of 'Large-section rectangular concrete filled tube',8 means the thickness is 8mm; H1 is the type number of distributive beam with section H200×100×10×10, H1+D1 means distributive beam together with inner ring diaphragm D1 (40×10); S means stiffening ribs with size of 100×6; LRCFT-10-H2-2 and LRCFT-10-H2-3 are comparing specimens for LD? and LD?; LRCFT-10-H3-1 and LRCFT-10-H3-2 are repeating specimens.

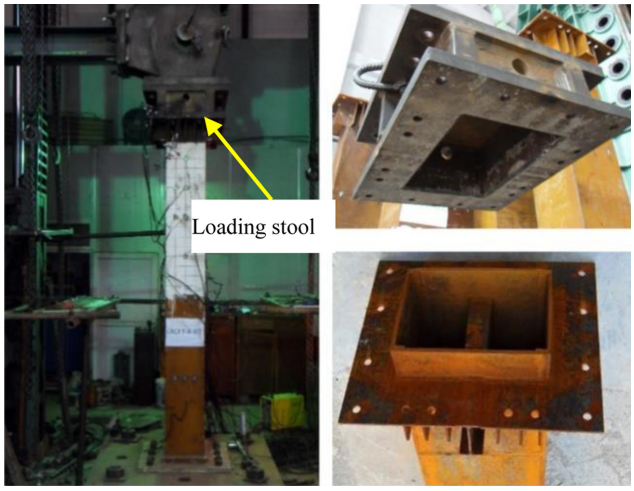

Figure 3. Test Set-up of Specimens with Load Detailings for Group 1 and 2.

diaphragm and vertical stiffeners were used, and the bottom of loading stool and the top diaphragms of specimens were bolted together with a clearance of 100 mm between the loading stool and the core concrete in order to make sure that the load can merely be acted to the steel tube. So the force pass here is "vertical load → loading stool → LD① → steel tube", and the core concrete will bear the load indirectly by the transferring detailings.

It is proven by testing that the vertical stiffening ribs below the horizontal diaphragm have a "clamp effect" on the steel tube (see Fig. 4), which may increase a confined effect, and contribute to the bonding effect between the tube inner surface and the concrete indirectly.

In order to reduce the "clamp effect", loading detailings LD② as shown in Fig. 5(a), together with the oiling of the inner face of tube, were adopted to the specimens in Group 3. A force sensor was placed at the opening bottom end of specimens, as shown in Figs. 5(b) and (c), to directly measure the force borne by the core concrete. So the force pass in these cases is "vertical load → loading stool → LD② → steel tube", and the test set-up is shown in Fig. 5.

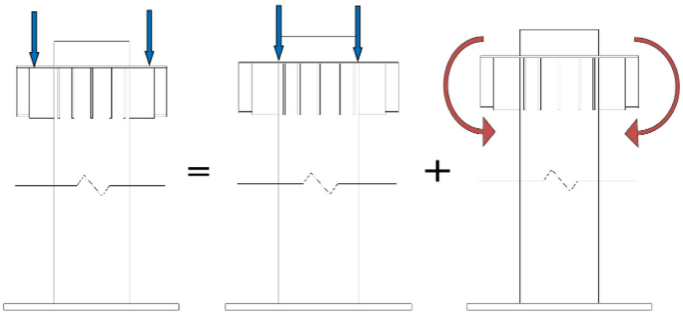

Figure 4. Clamp Effect of Vertical Stiffening Ribs below the Horizontal Diaphragm.

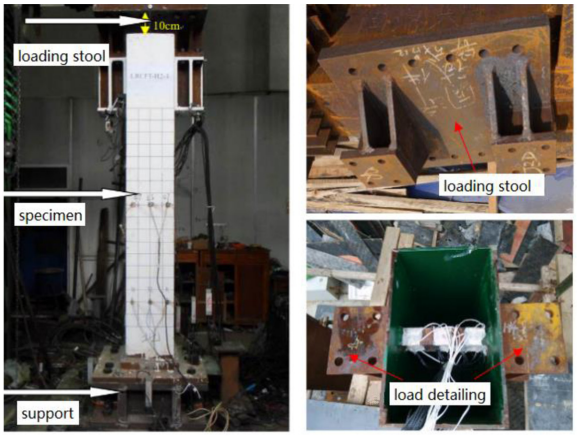

(a) Test setup of specimen of batch 3

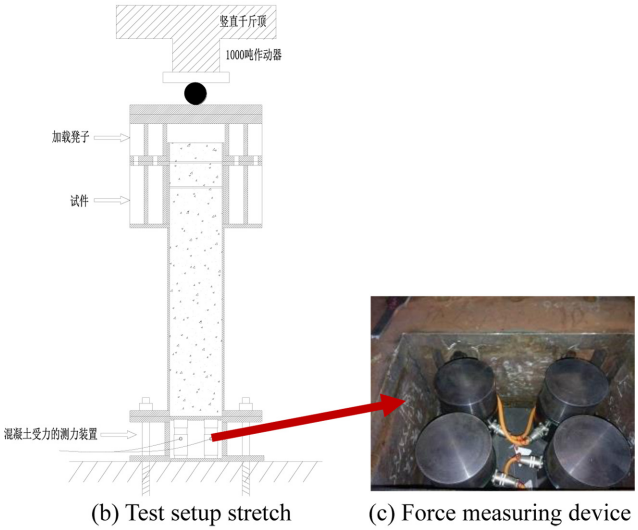

(b) Test setup stretch (c) Force measuring device

Figure 5. Test Setup of Specimens with Load Detailings for the Third Series of Specimens.

2.2. Test Results

The failure modes of the axial compression specimens are shown in the Figs. 7-9, and the corresponding capacities are listed in Table 2. Several conclusions can be drawn as follows: 1) The failure modes of specimens without loading detailing, LRCFT-6-1 and LRCFT-6-2, were both buckling at the steel tube under compression load, and some local buckling waves appeared continually in the vertical direction. The buckling deformation is more obvious at the top of the tube close to the welded vertical stiffeners. As for the core concrete, it was not crushed, and the ultimate capacity is close but smaller than the full yield force of the steel tube, which means that all the load was transferred to the steel tube, and the core concrete

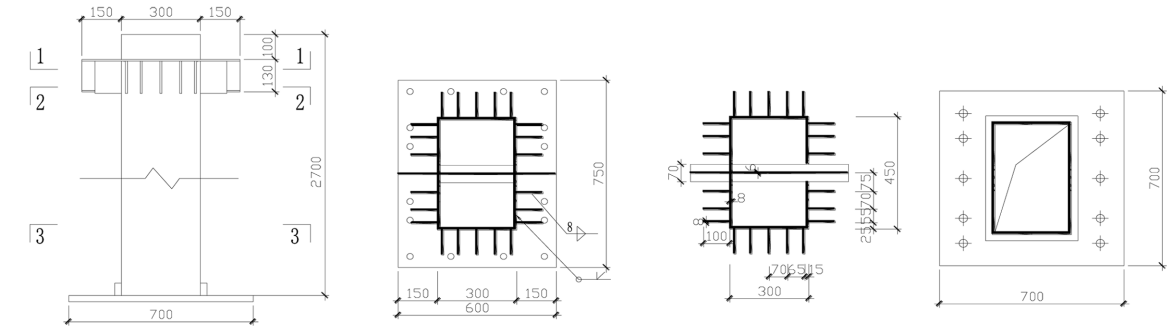

(a) Specimen LRCFT-8-H2

5

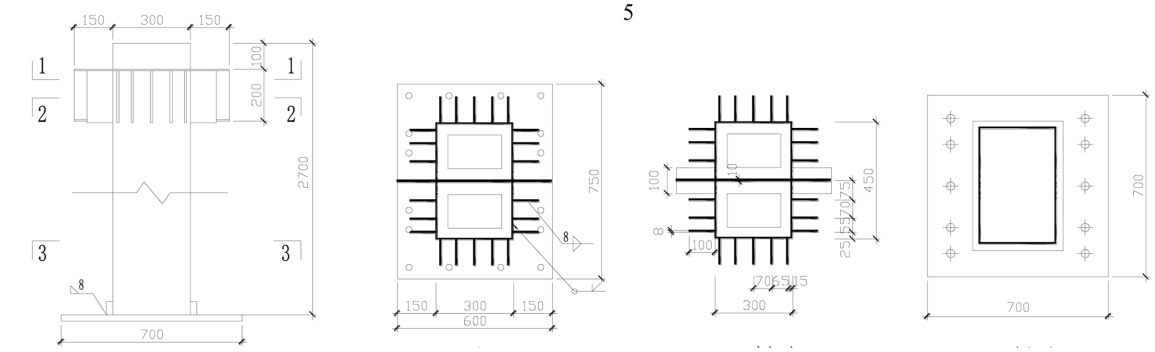

(b) Specimen LRCFT-6-H1+D1

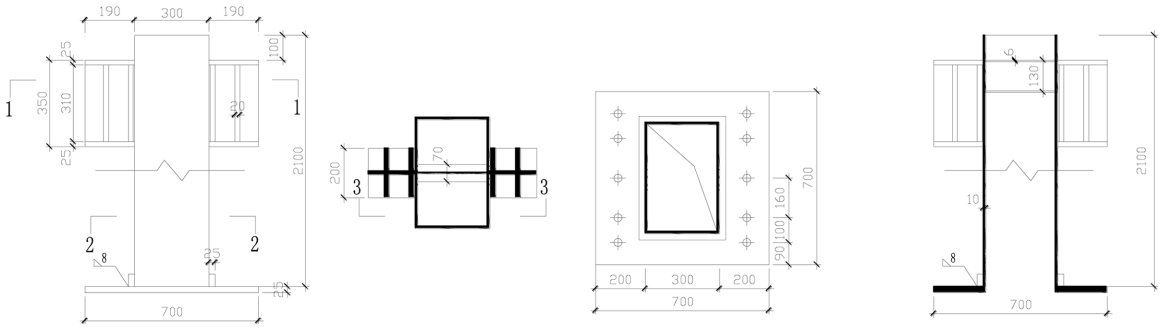

(c) Specimen of LRCFT-10-H4

Figure 6. Design Drawing of Typical Specimens.

almost bore no load. 2) The failure modes with LD① were mainly local buckling at random positions under compression load, but all the failure appeared at the top half part of the specimens. Whether the core concrete is crushed or not depends on the section of the distributive beam, as well as the "clamp effect" due to the loading detailings. For example, specimen LRCFT-10-H1, with distributive beam section H200×100×10×10 was crushed, while specimen LRCFT-10-H2, with distributive beam section H130×70×6×6 was not. 3) The failure modes with LD② were mainly local buckling and the core concrete was not crushed, the position of local buckling mainly appeared at the wider plate under the loading beam. 4) The failure modes of the specimen with both distributive beam and inner ring diaphragm were local buckling at the steel tube with continual waves along the height of specimen, and all the core concrete was crushed. 5) Both ends of the distributive beam yielded because of the shear force, and the plastic deformation mainly formed in the shear yield stage and the deformation of other zones outside yielding ends of the distributive beam was unobvious; throughout slit appeared at the web and both flanges plates of distributive beam in some specimens. 6) There was no obvious plastic deformation in the specimens with both the distributive beam and the inner ring diaphragm, as shown in Fig. 8(d).

It can be found that, the capacity of specimens without any load transferring detailings is smaller than the full section yielding force of the steel tube only, and the co-working performance of steel tube and core concrete was unsatisfactory; while the capacity of specimens with the distributive beam or both the distributive beam and the

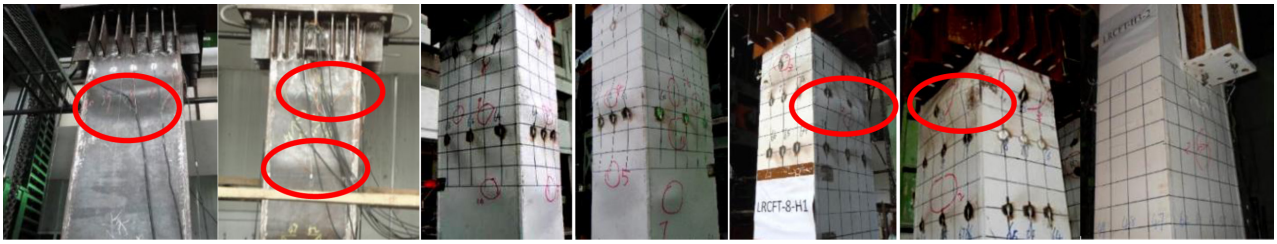

(a) LRCFT-6-1 (b) LRCFT-6-H1+D1 (c) LRCFT-6-H1+D1-S (d) LRCFT-8-H1 (e) LRCFT-10-H1 (f) LRCFT-10-H3-2

Figure 7. Failure Modes of Typical Specimens.

(a) LRCFT-6-1 (b) LRCFT-6-H1+D1 (c) LRCFT-6-H1+D1-S (d) LRCFT-8-H1 (e) LRCFT-10-H1 (f) LRCFT-10-H3-2

Figure 8. Failure Modes of Core Concrete of Typical Specimens.

(a) LRCFT-10-H2-2 (b) LRCFT-10-H2-3 (c) LRCFT-10-H3-1 (d) LRCFT-6-H1+D1-S

Figure 9. Failure Modes of Load Transferring Detailings.

inner ring diaphragm is far beyond the full section yielding capacity of the steel tube only, which means the co-working performance is obviously improved by the load transferring detailings. The ultimate axial compression capacity of specimens with the distributive beam and the inner ring diaphragm can be 85% of the nominal strength even the local buckling occurred before full section yielded due to large width to thickness ratio. Therefore, the efficiency of the load transfer detailings has been established, and the purpose of design can be realized.

Specimens of Group 2 was tested in order to investigate the effect of the distributive beam on a vertical load transfer and axial compression performance. The core concrete of specimen LRCFT-10-H1 and LRCFT-8-H1 was crushed, while the core concrete of specimens LRCFT-10-H2 and LRCFT-8-H2 was not, but the shear failure appeared on the distributive beam at both ends. Although the shear stiffness of H130×70×6×6 is far below H200×100×10×10, both specimens were able to reach 90% of the nominal capacity, which means a distributive beam even with relatively smaller stiffness can still be efficient in load transfer requirement. There was obvious slide deformation at the top of specimens between steel tube and core concrete, and the main reason is due to plastic deformation of the distributive beam, which lead tube and core concrete do not meet the plane-section assumption. Generally, in aspect of the failure mode and axial compression capacity, it's an efficient method to transfer load to core concrete by setting the distributive beam. Moreover, the ultimate capacity of specimen LRCFT-6-S-1 is far beyond specimen without stiffeners, which reached 1.26N_u (N_u=f_yA_s+$f_{ck}A_c$=6727.6 kN).

It had been proven that the distributive beam can transfer axial load to core concrete directly and efficiently, and the detailing with both the distributive beam, and the inner ring diaphragm can ensure the plane-section assumption for such a large-section CFT.

Table 2. Axial Compression Capacity of Specimens

Specimens No.	Steel strength f_y (MPa)	Concrete strength f_{ck} (MPa)	Initial bulking load N_i (kN)	Ultimate capacity N_u (kN)	Nominal capacity N_0 (kN)	Failure mode of distributive beam	Core concrete
LRCFT-6-1	380.3	43.9	-	3274	8905	-	-
LRCFT-6-2	380.3	43.9	-	2721	8905	-	-
LRCFT-6-H1	380.3	43.9	-	6509	8905	plastic failure	-
LRCFT-6-H1+D1	380.3	43.9	-	8003	8905	elastic, no obvious deformation	crushed
LRCFT-6-H1+D1-S	286.8	33.2	8367	8507	7072	elastic, no obvious deformation	crushed
LRCFT-8-H1	290.9	33.2	5568	7700	7508	plastic failure	plastic crack
LRCFT-8-H2	290.9	33.2	4978	6628	7508	plastic failure	-
LRCFT-10-H1	289.1	33.2	7098	9022	8218	plastic failure	crushed
LRCFT-10-H2-1	289.1	33.2	6892	8009	8218	plastic failure	-
LRCFT-10-H2-2	355.5	33.0	7319	7873	9163	plastic failure	-
LRCFT-10-H2-3	355.5	33.0	4738	6291	9163	plastic failure	-
LRCFT-10-H3-1	355.5	33.0	4953	7035	9163	plastic failure	-
LRCFT-10-H3-2	355.5	33.0	5485	7097	9163	plastic failure	-
LRCFT-10-H4	355.5	33.0	4878	5790	9163	plastic failure	-
LRCFT-10-H5	355.5	33.0	4555	6347	9163	plastic failure	-

Note: According to Chinese code, nominal capacity $N_0 = f_y A_s + f_{ck} A_c$, where, f_y is the actual yield strength of steel, A_s is the area of steel section, f_{ck} is the actual concrete axial compressive strength, A_c is the area of core concrete.

Table 3. Parameters of Specimens

Specimen No.	Section (mm)	Width to Thickness Ratio w/t	Stiffeners	Stiffener section (mm)
AC75-N	450×300×6×6	75	-	-
AC75-I60	450×300×6×6	75	I	60×4
AC75-T20	450×300×6×6	75	T	20×4
AC75-T25	450×300×6×6	75	T	25×4
AC75-T30	450×300×6×6	75	T	30×4
AC75-TT25	450×300×6×6	75	two T	25×4
AC75-TT16	450×300×6×6	75	two T	16×4
AC112-N	450×300×4×6	112.5	-	-
AC112-T20	450×300×4×6	112.5	T	20×4
AC112-TT25	450×300×4×6	112.5	T	25×4
AC112-TT16	450×300×4×6	112.5	T	16×4

Note: 'AC' is axial compression, 'N' means no stiffener, 'I' means I-shaped, 'T' means T-shaped, 'TT' means two T-shaped stiffeners.

3. Research on CFTs with T-Shaped Stiffeners to Improve Local Buckling Capacity

3.1. Specimens and Test Set-up

The specimen section is 450mm×300mm with reduced scaled ratio 5:1, as same as before. The stiffeners were welded to the inner wider panel of the steel tube, i.e., panels with 450mm wide. The height of specimens is 1500mm to avoid integral buckling. All the specimens were tested under axial compression load.

The limitation of width to thickness ratio of a panel is $60\sqrt{235/f_y}$ according to Chinese composite structure code, the steel strength is Q345B, so the limitation ratio is 50. In order to investigate the influence of T-shaped on large width to thickness ratio panels, 4 mm and 6 mm thick panels were adopted, which means the width to thickness ratio is 112.5 and 75. In this paper, three types of T-shaped stiffeners were studied with specimens without stiffener and one with a common I-shaped stiffener as comparison. The parameters of specimens are shown in Table 3, and test set-up is shown in Fig. 10 as below.

3.2. Test Results

The failure modes of stiffened specimens are shown in Fig. 11 and the capacities measured are listed in Table 4. The results indicate that: 1) for the specimens of AC75 series, only small buckling deformation appeared before the specimen reached their ultimate capacities. When the specimens reached the ultimate capacity, core concrete was crushed and pushed the tube panel outwards; 2) for the specimens of AC112 series, buckling deformation is obvious before load reached the ultimate capacity due to

Figure 10. Set-up of Axial Compression Specimen.

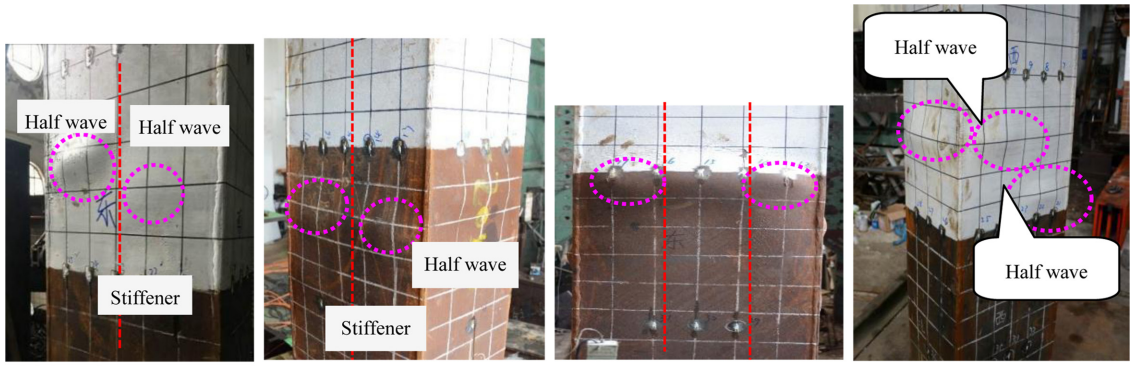

Figure 11. Failure Modes of T-shaped Stiffeners under Axial Compression Load.

the large width to thickness ratio; 3) the buckling waves of tube panels is mainly separated by longitudinal stiffeners, which indicated that the stiffeners can fix panel to the concrete and increase the critical buckling stress; 4) for the specimens of AC112 with two stiffeners, buckling mode combined with separated sub-panel buckling and entire panel buckling, it means the stiffness of the T-shaped stiffener is not sufficient to resist panel from bulking outwards. but it can increase the critical stress to some degree; 5) the efficiency of T-shaped stiffeners is better than the common I0shaped stiffeners, and the concrete constrained by the flange of T-shaped stiffeners can provide additional bending stiffness by forming a composite section.

Table 4. Load Bearing Capacity of Axial Compression Specimens

Specimens No.	N_0 (kN)	N_u (kN)	N_b (kN)	N_c (kN)	Phenomena
AC75-N	7294.1	7224	4820	4082	buckling to outside
AC75-I60	7294.1	8298	5340	4756	double half waves very obviously
AC75-T20	7294.1	8568	5780	5110	double half waves, but not so obviously
AC75-T25	7294.1	8727	6200	4462	double half waves obviously
AC75-T30	7294.1	8030	6300	4939	double half waves obviously
AC75-TT25	7294.1	8494	5700	5599	three half waves very obviously
AC75-TT16	7294.1	8306	6650	-	three half waves, but not so obviously
AC112-N	6604.2	6195	2570	4089	buckling to outside
AC112-T20	6604.2	6797	3920	3890	double half waves very obviously
AC112-TT25	6604.2	7315	3705	4543	three waves very obviously
AC112-TT16	6604.2	6783	3300	4809	three waves, but not so obviously

Note: N_0 is the nominal capacity, $N_0=f_yA_s+f_{ck}A_c$; N_u is the actual capacity in test, N_b is critical bulking stress of wider panels. N_c is force borne by concrete.

Table 5. Typical Section Size of Rectangular CFT Columns used in Baoneng GFC

Stories	Length × Width (mm)
1-10	5200 × 3500
11-32	4800 × 3300
33-63	4500 × 3000
64-82	4200 × 2650
83-101	3600 × 2400
102-108	3000 × 2000
109-112	2000 × 2000

4. Case Study

The two construction detailings mentioned above in this paper have been used in the "Shenyang Baoneng Global Financial Center" in Shenyang, China, as shown in Fig. 12. As a super high-rise building, rectangular CFT columns with large-section, as shown in Table 5 were used in the structural system to bear huge vertical load. Steel ratios of large-section columns can be reduced from 6.3-7.8% to 4.0-6.1% by using the T-shaped stiffeners, which means approximately 30% of steel of columns can be saved (5000 t).

Figure 12. Shenyang Baoneng Global Financial Center, Baoneng GFC.

5. Conclusions

In order to increase the load transferring performance of large-section CFT column joints and guarantee large width to thickness ratio not to buckling before the ultimate capacity, two new types of construction detailings, a distributive beam together with the inner ring diaphragm and longitudinal stiffeners were checked. Test results have shown that these two detailings can optimize performance of large-section CFT components and result in an economical steel cost. it can be concluded from this research that:

1) Comparing the failure mode and the capacity between the specimens with and without setting the distributive beam, it is shown that the distributive beam can transfer vertical load to core concrete directly apart from merely bond force between steel inner face and concrete. This type of detailing ensures the co-working performance of two materials and the plane-section assumption at the joint zone of CFT columns, which results in a high ultimate capacity.

2) It was shown that the function of the distributive beam is to transfer the vertical load from outer panels to core concrete, the different displacement between the steel tube and the core concrete at the top of the columns is due to the plastic deformation and the shear failure of both end of the distributive beam. As the size of the distributive beam increases, more vertical load is transferred to the inner concrete.

3) Using the T-shaped stiffener welded to the inner face

of panels with large width to thickness ratio can enhance the local buckling stress significantly, and the failure mode changes from the whole panel buckling to sub-panel buckling separated by the stiffeners. It is an efficient approach to guarantee the local stability by using large width to thickness ratio panel beyond the specification limitation. The use of this type of detailings can result in an economical steel cost and offer convenience for welding procedures.

4) Multiple stiffeners are suggested to be set to the panel with width to thickness ratio far beyond the limitation, and the stiffeners can be taken as fixed pin-boundaries to the sub-panels.

References

American Concrete Institute. (2005). Building Code Requirements for Reinforced Concrete (ACI 318- 05)[S]. Detroit.

Architectural Institute of Japan (AIJ). (1997). Recommendations for Design and Construction of Concrete Filled Steel Tubular Structures [S].

Architectural Institute of Japan (AIJ). (2001). Standard for Structural Calculation of Steel Reinforced Concrete Structure, 5th Ed. [S], Japan.

Desmond, T. P., Pekoz, T., and Winter, G. (1981). Intermediate stiffeners for thin-walled members [J]. Journal of Structural Engineering, ASCE, 107(4), 627-647.

Goto, Y., Mizuno, K., and Kumar, G. P. (2012). Nonlinear finite element analysis for cyclic behavior of thin-walled stiffened rectangular steel columns with in-filled concrete [J]. Journal of Structural Engineering, 138(5).

Huang, H., Zhang, A., Li, Y., and Chen, M. (2011). Experimental research and finite element analysis on mechanical performance of concrete-filled stiffened square steel tubular [J]. Journal of Building Structures, 32(02), 75-82. (in Chinese)

Lee, K. C. and Yoo, C. H. (2012). Longitudinal stiffeners in concrete-filled tubes [J]. Journal of Structural Engineering, 138(6).

Luo, J., Li, Y., Zhang, Y., and et al. (2014). Experimental research on axial compression load transfer of large rectangular-section CFT columns with distributive beam embedded in beam-column joints [J]. China Civil Engineering Journal, 47(10), 50-60. (in Chinese)

Mohurd of P.R.C. GB 50936-2014 Technical Code for Concrete Filled Steel Tubular Structures [S]. Beijing, 2014.

Rhodes, J. (1984). Some thoughts on future cold-formed steel design rules [C]. Behaviour of Thin-Walled Structures, London. pp. 125-142.

Shen, Z. (2013). Research on co-work of steel and concrete of large section CFT columns. Tianjin University. The 13th National Modern Structural Engineering Symposium [C]. Tianjin University. (in Chinese)

Tao, Z. and Yu, Q. (2006). New Type of Composite Structure Columns [M]. Beijing: Science Press. (in Chinese)

Wang, D. (2006). Mechanical property of Thin-Walled Concrete-Filled Steel Tubular with Stiffen Ribs [D]. Fuzhou: Fuzhou University. (in Chinese)

Zhang, Y. and Chen, Y. (2006). Experimental study and finite element analysis of square stub columns with straight ribs of concrete-filled thin-walled steel tube with straight ribs of concrete-filled thin-walled steel tube [J]. Journal of Building Structures, 27(05), 16-22. (in Chinese)

Zhang, Y., Li, Y., Luo, J., and et al. (2014). Experimental study on load-carrying behavior of large-section CFT columns with distributive beam and inner diaphragm detailing in joints under compressing and bending loads [J]. China Civil Engineering Journal, 47(11), 45-54. (in Chinese)

Zhang, Y., Li, Y., Luo, J., and Fu, X. (2016). Compression load transfer mechanism of distributive beam detailings in large-section CFT columns (I): Experiment study [J]. China Civil Engineering Journal, 49(11), 1-10. (in Chinese)

Zhang, Y., Luo, J., Li, Y., and Fu, X. (2016). Compression load transfer mechanism of distributive beam detailings in large-section CFT columns (II): Numerical simulation [J]. China Civil Engineering Journal, 49(12), 16-26. (in Chinese)

Zhang, Y., Luo, J., Li, Y., and Shen, Z. (2016). State of the arts of load transfer mechanism between concrete core and steel tube in CFST [J]. Progress in Steel Building Structures, 18(3), 1-9. (in Chinese)